Advances in Silicon Science 4
Series Editor: J. Matisons

Michael J. Owen
Petar R. Dvornic *Editors*

Silicone Surface Science

Springer

Advances in Silicon Science

ADVANCES IN SILICON SCIENCE

VOLUME 4

Series Editor:

JANIS MATISONS
Gelest Inc., 11 East Steel Road, Morrisville, PA 19067, USA

Advances in Silicon Science is a book series which presents reviews of the present and future trends in silicon science and will benefit those in chemistry, physics, biomedical engineering, and materials science. It is aimed at all scientists at universities and in industry who wish to keep abreast of advances in the topics covered.

Series Editor

Prof. Janis Matisons
Senior R & D Manager
Gelest Inc
11 East Steel Road
Morrisville
Pennsylvania 19067
USA
jmatisons@gelest.com

Volume 4

Silicone Surface Science

Volume Editors

Michael J. Owen
Petar R. Dvornic
Michigan Molecular Institute
Midland, MI
USA

For further volumes:
www.springer.com/series/7926

Michael J. Owen • Petar R. Dvornic
Editors

Silicone Surface Science

Springer

Editors
Michael J. Owen
Michigan Molecular Institute
Midland, MI
USA

Petar R. Dvornic
Michigan Molecular Institute
Midland, MI
USA

ISSN 1875-3108
ISSN 1875-3086 (electronic)
Advances in Silicon Science
ISBN 978-94-007-3875-1
ISBN 978-94-007-3876-8 (eBook)
DOI 10.1007/978-94-007-3876-8
Springer Dordrecht Heidelberg New York London

Library of Congress Control Number: 2012939196

Printed on acid-free paper

Springer is part of Springer Science+Business Media (www.springer.com)

Preface

God made the bulk; surfaces were invented by the devil
Wolfgang Pauli[1]

It is somewhat surprising, in our opinion, that this book, to the best of our knowledge, is the first to be devoted to the surface properties and behavior of silicone polymers. The situation is all the more perplexing when one considers that surface-related applications have consistently accounted for the major part of the commercial success of silicones since the establishment of this industry in the early 1940s.

The importance of surfaces and interfacial phenomena cannot be overemphasized. When any two materials are brought together it is their surfaces that initially matter and their interfacial interactions that need to be studied and understood first. Therefore, in order to contribute to this, in this book we attempt to present a broad overview of the state-of-the-art of silicone surface science by a group of widely recognized experts in their fields summarizing both the historical development and the current progress in each selected area. With almost 70 years of scientific and technological interest in silicones we can hardly claim to be rigorously comprehensive, but we are sure that the most exciting developments in this field today are covered in this volume.

Much of the content of this book deals with polydimethylsiloxane (PDMS) since it has been the mainstay of the silicone industry from its very beginnings to the present day. Furthermore, looking into the future, while anticipating continued interest in and development of other polymers derived from organosilicon entities, there is no reason not to believe that the science and applications of PDMS and related organosiloxane polymers will continue to grow and play as important a role as they have in the past.

As is common in the field of silicon-containing polymers, we use the term silicone to describe polymers whose backbone is siloxane, i.e. alternating arrangement of silicon and oxygen atoms, with pendent organic groups attached to that backbone. Consequently, polyhedral oligomeric silsesquioxanes (POSS), which certainly meet

[1] Quoted in "*Growth, Dissolution and Pattern Formation in Geosystems*" (1999) by Bjorn Jamtveit and Paul Meakin, p. 291.

the "alternating siloxane bonds" requirement, are not usually considered "silicones", because of their insufficient molecular weights and fundamentally different macroscopic properties. Nevertheless, we consider these oligomers to be a proper subject for inclusion in this volume because of their critical importance to silicone surface science as explained in detail in two chapters dealing with POSS derivatives.

What might appear to some to be a somewhat capricious chapter order is based on our attempt to marry two seemingly "incompatible" concepts: (i) a progressive shift from fundamentals to more applied topics, and (ii) a development from "pure" PDMS to other important, surface-active silicones such as fluorosilicones and modified materials such as surfactants and coupling agents. The book opens with a general introduction to silicone surfaces with an emphasis on the surface properties of PDMS. Following this, in Chap. 2 Ahn and Dhinojwala describe the sum frequency generation vibrational spectroscopy of silicone surfaces and interfaces, a relatively recently introduced technique that has provided considerable new insight into surface structure and most notably to buried interfaces as well. Genzer and co-workers have made great strides in creating different functionalities on silicone surfaces and their contributions are reviewed in Chap. 3. Superhydrophobic surfaces have featured strongly in the last decade, and McCarthy et al. review their silane/siloxane studies of this topic in Chap. 4. Chapters 5 and 6 deal with fluorine-containing silicones where Ganachaud and Ameduri and their colleagues review structure/property relationships in fluorosilicones and Tuteja and Mabry contribute a chapter on fluoro-POSS materials which are highly relevant to the earlier topic of superhydrophobicity, respectively. Our strong interest in fluorosilicones derives from their potential to produce significantly lower surface energies than conventional PDMS surfaces.

Langmuir trough investigations of silicones have been of interest since surface studies of silicones began. In Chap. 7 Esker and Yu provide a summary of this topic with an update of recent works that offers another facet of the growing importance of POSS compounds to organosilicon surface science today. A topic of high-interest to current siloxane science with considerable surface-related implications is the interaction of proteins and silicon-based materials which is the subject of Chap. 8 by Clarson and co-workers. This is followed by a review of silicone surfactant fundamentals and applications by Snow and Petroff in Chap. 9, while Matisons' Chap. 10 deals with the adsorption of polymeric siloxanes on glass surfaces and their coupling behavior as well as with more conventional silane coupling agents. Surface treatments such as plasma and corona have been widely exploited in silicone surface modification. These are summarized in Chap. 11 by Hillborg and Gedde (see also Chap. 3 which deals with aspects of this topic).

Analytical techniques are self-evidently central to understanding of silicone surface behavior. A review of these studies with emphasis on X-ray photoelectron spectroscopy (XPS), secondary ion mass spectrometry (SIMS), scanning electron microscopy (SEM) and scanning probe microscopy (SPM) is provided by Leadley, O'Hare and McMillan in Chap. 12. Finally, we close with an outline of some important surface applications of silicones relating to both the science and technology of silicone surfaces. Some of these applications are also included in several of the earlier chapters, underlining a dominant theme of this book, the relationship between

the structure and surface properties of silicones and their utilization in various everyday as well as more sophisticated applications.

A variety of authors contributed different perspectives to this work, including academic and industrial specialists from Europe and North America. We sincerely thank all of them for their impressive contributions and their patience and perseverance throughout the process of bringing this book to fruition. We are particularly grateful to our publishing editor, Dr. Sonia Ojo and her Springer colleagues for their expert help during the preparation of the manuscript and to Donatas Akmanavičius of VTeX UAB in the realization of this finished work.

Midland, MI, USA

Michael J. Owen
Petar R. Dvornic

Contents

Contributors

Dongchan Ahn Dow Corning Corporation, Midland, MI, USA

Bruno Ameduri Institut Charles Gerhardt, Equipe "Ingénierie et Architectures Macromoléculaires", UMR5253 CNRS, ENSCM, Montpellier Cedex, France

Stephen J. Clarson Department of Chemical and Materials Engineering and the Polymer Research Center, University of Cincinnati, Cincinnati, OH, USA

Julie A. Crowe-Willoughby Department of Chemical & Biomolecular Engineering, North Carolina State University, Raleigh, NC, USA; College of Textiles, North Carolina State University, Raleigh, NC, USA

Ali Dhinojwala Department of Polymer Science, The University of Akron, Akron, OH, USA

Petar R. Dvornic Michigan Molecular Institute, Midland, MI, USA

Kirill Efimenko Department of Chemical & Biomolecular Engineering, North Carolina State University, Raleigh, NC, USA

Alan R. Esker Department of Chemistry (0212), Virginia Tech, Blacksburg, VA, USA

Alexander Y. Fadeev Polymer Science and Engineering Department, University of Massachusetts, Amherst, MA, USA

Kathy Gallardo Department of Chemical and Materials Engineering and the Polymer Research Center, University of Cincinnati, Cincinnati, OH, USA

François Ganachaud Institut Charles Gerhardt, Equipe "Ingénierie et Architectures Macromoléculaires", UMR5253 CNRS, ENSCM, Montpellier Cedex, France; IMP@INSA, UMR5223 CNRS, INSA-Lyon, Villeurbanne Cedex, France

Lichao Gao Polymer Science and Engineering Department, University of Massachusetts, Amherst, MA, USA

Ulf W. Gedde Fibre and Polymer Technology, School of Chemical Science and Engineering, Royal Institute of Technology, Stockholm, Sweden

Jan Genzer Department of Chemical & Biomolecular Engineering, North Carolina State University, Raleigh, NC, USA

Larry Grazulis University of Dayton Research Institute, Dayton, OH, USA

Siska Hamdani-Devarennes Institut Charles Gerhardt, Equipe "Ingénierie et Architectures Macromoléculaires", UMR5253 CNRS, ENSCM, Montpellier Cedex, France; Ecole des Mines d'Alès, CMGD, Alès, France

Henrik Hillborg Fibre and Polymer Technology, School of Chemical Science and Engineering, Royal Institute of Technology, Stockholm, Sweden; Corporate Research, ABB AB, Västerås, Sweden

Joseph W. Krumpfer Polymer Science and Engineering Department, University of Massachusetts, Amherst, MA, USA

Stuart Leadley Dow Corning Europe, Seneffe, Belgium

Claire Longuet Ecole des Mines d'Alès, CMGD, Alès, France

Joseph M. Mabry Space and Missile Propulsion Division, Air Force Research Laboratory, Edwards AFB, CA, USA

Janis G. Matisons Gelest Inc., Morrisville, PA, USA

Thomas J. McCarthy Polymer Science and Engineering Department, University of Massachusetts, Amherst, MA, USA

Christopher McMillan Dow Corning Corporation, Midland, MI, USA

Lesley-Ann O'Hare Dow Corning Corporation, Midland, MI, USA

Michael J. Owen Michigan Molecular Institute, Midland, MI, USA

Ali E. Őzçam Department of Chemical & Biomolecular Engineering, North Carolina State University, Raleigh, NC, USA

Cedric Pasquet Institut Charles Gerhardt, Equipe "Ingénierie et Architectures Macromoléculaires", UMR5253 CNRS, ENSCM, Montpellier Cedex, France; IMP@INSA, UMR5223 CNRS, INSA-Lyon, Villeurbanne Cedex, France

Siddharth V. Patwardhan Department of Chemical and Process Engineering, University of Strathclyde, Glasgow, UK

Lenin J. Petroff Dow Corning Corporation, Midland, MI, USA

Steven A. Snow Dow Corning Corporation, Midland, MI, USA

Anish Tuteja Department of Materials Science and Engineering, University of Michigan, Ann Arbor, MI, USA

Hyuk Yu Department of Chemistry, University of Wisconsin, Madison, WI, USA

Chapter 1
General Introduction to Silicone Surfaces

Michael J. Owen and Petar R. Dvornic

1.1 Introduction

Surface properties of silicones have been exploited from the start of the silicone industry and continue to be dominant today. According to Warrick [1] one of the most useful early applications was the treatment of glass fibers using hydrolyzed silanes to create a water-repellent product. Other early silicone products include hydrophobic greases to seal aircraft ignition systems and antifoam agents for petroleum oils. We conservatively estimate that 70 % of the current market for silicones result from their surface properties and behavior. For more information on silicone applications see Chap. 13.

The term "silicone" is not a precise one. We use it to describe polymeric materials based on a silicon-oxygen backbone with organic groups attached directly to silicon atoms. These organic groups can be inert or reactive so our definition encompasses not only polydimethylsiloxane $-[Si(CH_3)_2O]_n-$ (PDMS), which continues to hold the dominant position in the silicone industry, but also other polysiloxanes such as fluorosilicones and hydrolyzed silane coupling agents. This definition does not include, nor does this volume address except in passing, other organosilicon polymers such as polycarbosilanes, polysilanes and polysilazanes. With its inorganic backbone and organic pendant groups, PDMS and other silicone polymers belong to the class of "semi-inorganic" [2] or "organo-inorganic" polymers. Superficially, the surface properties of PDMS might be expected to be an average of these two dissimilar constituents but this is not the case. For example, the surface energy and hydrophobicity of PDMS are much more akin to hydrocarbons such as paraffin wax than they are to silica. The explanation lies in two general rules, namely, the second

M.J. Owen (✉) · P.R. Dvornic
Michigan Molecular Institute, 1910 W. St. Andrews Rd., Midland, MI 48640, USA
e-mail: michaelowen01@chartermi.net

P.R. Dvornic (✉)
e-mail: dvornic@mmi.org

M.J. Owen, P.R. Dvornic (eds.), *Silicone Surface Science*, Advances in Silicon Science 4,
DOI 10.1007/978-94-007-3876-8_1,

law of thermodynamics and Langmuir's principle of the independence of surface action [3].

The second law of thermodynamics can be expressed in numerous ways. One common form is that systems will change spontaneously in the direction of minimum total free energy. Hence, for a polymer like PDMS containing both polar and non-polar entities it is axiomatic that the low-surface-energy methyl groups will accumulate in the surface and dominate surface behavior. Langmuir's principle takes this expectation a step further. It postulates that one can conceive of separate surface energies for each of the different parts of complex molecules and that the surface energy of a material made of such molecules is determined by the composition and orientation of the outermost groups independent of the underlying components. This is the principle on which Zisman [4] based his quantification of the surface energy of hydrocarbon and fluorocarbon groups showing that their contributions to the total surface energy of the material decrease in order: $–CH_2– > CH_3– > –CF_2– > –CF_3$. The principle is not absolute, but is a very good first approximation. Most measurements of solid surface energy by contact angle determination (discussed later in this chapter) attribute only a small polar component that would arise from the Si–O chain backbone to the surface energy of PDMS. Another example of particular relevance to fluorosilicones is the somewhat surprising longer range effect exhibited by the uncompensated dipole that arises at the junction of fluorocarbon and hydrocarbon entities.

Before considering surface properties of silicones in general and PDMS in particular, it is pertinent to consider the fundamental characteristics of PDMS that account for its pre-eminent position in the ranks of organo-inorganic polymers. These include:

- Low intermolecular forces between pendant methyl groups [$p^* = 341$ J cm^{-3}]
- Compact size of the methyl group [van der Waals radius = 200 pm]
- High siloxane backbone flexibility [$T_g = 150$ K]
- High siloxane bond energy [445 kJ mol^{-1}]
- Partial ionic nature of the siloxane bond [*ca* 40 % ionic]

Here p^* is the characteristic pressure obtained from the Shih and Flory equation of state [5] and it is a measure of intermolecular energy per unit volume, which has a reasonable correlation with surface energy, and T_g is the temperature of the glass transition. The first three of the above characteristics together explain much of the surface and bulk physical behavior of PDMS with the other two accounting for the chemical consequences of environmental exposure in use [6]. In principle, all applications of silicones can be directly linked to combinations of these five factors, an exercise that is the subject of Chap. 13. The use of "high" and "low" as descriptors in this list is in qualitative comparison to other organic polymers in general. For example, when considering the intermolecular forces between polymer chains or segments, the range is from strongly polar hydrophilic materials such as polyacrylamide to low-surface-energy aliphatic fluoropolymers. PDMS lies low on this scale in the region between hydrocarbons such as polypropylene and fluoropolymers such as polytetrafluoroethylene.

Table 1.1 Glass transition temperatures of selected polysiloxanes and other polymers

Polymer	T_g (K)
Polypentamethylcyclopentasiloxane (PD_5)	122 [7]
Polydiethylsiloxane	134 [8]
Polymethylhydrogensiloxane	135 [8]
Polymethylethylsiloxane	138 [8]
Co-poly(CF_2CF_2–O–CF_2O)	140 [9]
Polyethylene	148 [10]
Polydimethylsiloxane	150 [10]
Polydimethylsilmethylene	173 [10]
Polymethylnonafluorohexylsiloxane	198 [11]
Polyisobutylene	200 [10]
Polymethyltrifluoropropylsiloxane	203 [10]
Polyoxyhexafluoropropylene	207 [10]
Polydimethylphosphazene	227 [12]

A low T_g of a polymer segment reflects pronounced backbone chain flexibility (low energy barrier for rotation around the Si–O main chain bonds) although other factors, such as pendant group size also have an effect. PDMS benefits from both the compact size of the methyl groups (the smallest possible alkane substituent; only an atom such as hydrogen or fluorine is smaller) and the intrinsic flexibility of the siloxane backbone (the most flexible chain of atoms known to polymer science [13]). The architecture of the backbone, consisting of alternating small, unsubstituted oxygen atoms and larger, substituted silicon atoms also plays a part. Table 1.1 lists T_g values of selected polymers to put the PDMS value in perspective. Note that PD_5 is a polymer of D_5H, pentamethylcyclopentasiloxane reported by Kurian and co-workers [7] that consists of cyclopentasiloxane rings linked by siloxane linkages. Note also that the lowest reported fluoropolymer glass transition is for the fluoroether copoly(oxytetrafluoroethylene-oxydifluoromethylene), which has no pendant groups, only fluorine atoms.

The most important surface property of any polymer is its surface energy which arises directly and inevitably from the imbalance of intermolecular forces between the polymer molecules at any phase boundary. By surface energy we mean the surface free energy being the change in total surface free energy per unit change in surface area brought about by an expansion of the surface at constant temperature, pressure and number of moles of substance in the surface. In principle, these conditions can be met for a liquid polymer. The free energy per unit area is then numerically and dimensionally identical to the surface tension, expressed as a force per unit length in the surface. The SI unit for surface energy is $mJ\,m^{-2}$. Provided the viscosity is not too high, the liquid surface tension of a polymer can be directly measured, giving an unambiguous value if both the temperature of the measurement and the molecular weight of the sample are specified. The latter information is necessary as liquid surface tension of polymers is usually a function of molecular weight due

primarily to end-group effects. Surface tension values of liquids are usually quoted in $mN\,m^{-1}$, numerically equal to cgs dyne cm^{-1} units. For solid surfaces it is conventional to speak of surface energy (in $mJ\,m^{-2}$) rather than surface tensions. These two quantities are numerically equal. Both σ and γ are used as the symbols for surface tension and surface energy, but in this volume we choose the latter symbol.

For a solid polymer the situation is much more complex. The surface area cannot generally be changed at constant chemical potential to allow an equal number of moles to be present before and after expansion of a solid surface. Moreover, elastic forces complicate the issue and the surface state after extension can be far from equilibrium. Therefore, indirect approaches are usually resorted to for the determination of the surface energy of a solid. Historically, and still to a very great extent today, investigators resort to methods based on contact angle determinations most commonly using either a sessile drop or Wilhelmy plate configuration. In the sessile drop approach a liquid drop is simply placed upon a smooth, flat sample of the solid under investigation. In the Wilhelmy plate method a thin plate of the sample is partially immersed in a chosen liquid. A variety of liquids may be chosen to probe the surface and there is also a variety of semi-empirical equations available to convert the obtained contact angle data into surface energy values. The consequence of this is that the literature contains a variety of conflicting values for solid surface energy and the task of selecting a preferred value is challenging.

One way out of this dilemma is to resort to contact mechanics. Using methodology such as the Johnson, Kendall and Roberts (JKR) approach [14], one can obtain objective values of polymer surface energy. However, relatively few polymers have been characterized so far in this manner, but, fortunately, PDMS is among these, thanks primarily to the studies of Chaudhury and co-workers [15] and the fortuitous situation that its bulk properties are ideal for contact mechanics investigations. For all the above described reasons, in this chapter we first discuss the liquid surface tension of PDMS, then the contact angle of water on solid PDMS, followed by the determination of solid surface energy by contact angle and contact mechanics approaches. Langmuir trough studies are also briefly reviewed.

1.2 Liquid Surface Tension

Figure 1.1 [16] shows liquid surface tension (γ_{LV}) at 20 °C as a function of boiling point for low molecular weight linear PDMS and poly(oxyhexafluoropropylene) as well as *n*-alkanes and *n*-fluoroalkanes which can be viewed as oligomers of polyethylene (PE) and polytetrafluoroethylene (PTFE). At first glance these curves seem to parallel the familiar order, established half a century ago by Zisman and coworkers [4] for solids by contact angle study, where the CF_3– group has the lowest surface energy, followed by the –CF_2– group and the CH_3– group, with the –CH_2– group being the least surface active of these four entities. However, it appears that the PDMS and *n*-fluoroalkane curves might cross if higher liquid fluoroalkanes were available. There is also the impression that the oligomers with a flexibilizing oxygen linkage have a flatter slope than the alkanes and fluoroalkanes. A lower coefficient of property change with temperature is a familiar situation with PDMS, often at-

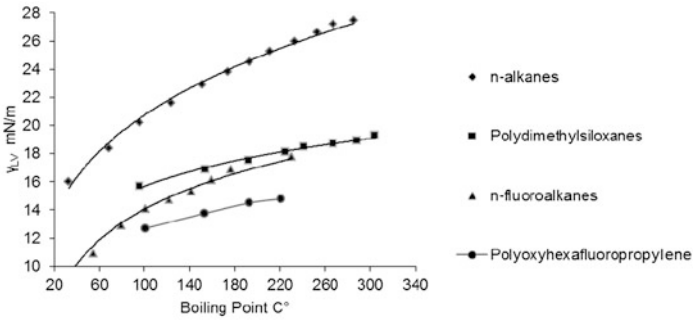

Fig. 1.1 Dependence of surface tension at 20 °C on boiling point for a variety of hydrocarbon- and fluorocarbon-containing compounds. Reprinted from Ref. [16] with kind permission of © The American Chemical Society (1980)

Table 1.2 Surface tensions and their temperature coefficients of selected liquids

Polymer	γ_∞ (mN m^{-1})	Temp. (°C)	$-\delta\gamma/\delta T$ (mN {m K}$^{-1}$)
Poly(oxyhexafluoropropylene)	18.4	25	0.059
n-fluoroalkanes (PTFE)	25.8	20	0.053
PDMS	21.3	20	0.048
PMTFPS	24.4	25	–
n-alkanes	36.9	20	0.060

tributed to its backbone flexibility but in this case possibly also a function of the varying end-groups of these four sets of oligomers.

The best way to remove complications of end-group, density and volatility effects is to extrapolate the data to infinite molecular weight. The LeGrand and Gaines equation [17] Eq. (1.1) offers a convenient way of doing this. Here γ_{LV} is again the surface tension of any given liquid polymer sample (LV indicating the value at the liquid (L)/vapor(V) interface) and γ_∞ is the extrapolated value at $1/M_n^{2/3} = 0$, where M_n is the number average molecular weight, and K is a constant. The extrapolation to zero reciprocal molecular weight is short, yielding convincing values shown in Table 1.2 together with the temperature (T) at which the measurements were made and the coefficient of surface tension change with temperature, $\delta\gamma/\delta T$.

$$\gamma_\infty = \gamma_{LV} - K/M_n^{2/3} \tag{1.1}$$

It can be seen from this table that γ_∞ for both the *n*-fluoroalkanes and polymethyltrifluoropropylsiloxane (PMTFPS) is higher than that of PDMS. For PMTFPS we can rationalize that the two CH_2 groups of higher intrinsic surface energy than CH_3 must more than outweigh the effect of the lower surface energy CF_3 group. The CF_3 group is insufficiently stable when directly attached to silicon for one to test this idea by dispensing with the ethylene bridge in PMTFPS and attempting to study $[Si(CH_3)(CF_3)O]_n$. The temperature coefficient values are not

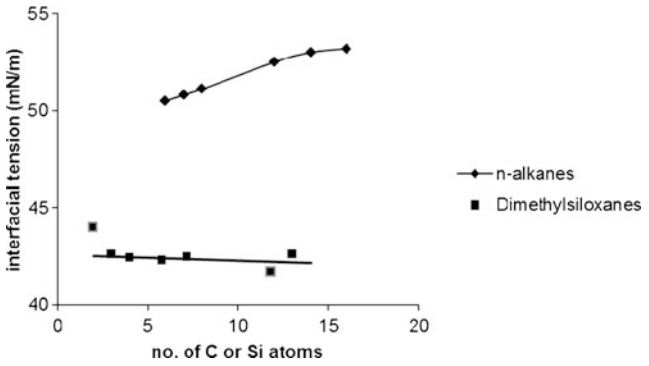

Fig. 1.2 Interfacial tensions of *n*-hydrocarbons and polydimethylsiloxane oligomers against water

at infinite molecular weight since insufficient data are available. Instead, the values chosen are for the highest molecular weight available. More details are given in the original citation [18]. Surface tensions of polymers vary linearly with temperature with $-\delta\gamma/\delta T$ values typically in the 0.05 to 0.08 range and the PDMS value being the lowest value reported. These values are somewhat lower than the temperature coefficients for non-polymeric liquids an effect that is attributed to conformational restrictions of long-chain molecules. Generally, increasing surface tension correlates weakly with increasing temperature coefficient, although this is not evident from the limited selection made in Table 1.2.

The interfacial tension between liquids can also be measured directly (see also Chap. 5, Appendix A.1). Water is usually the other phase of interest and Fig. 1.2 shows the interfacial tension between water and PDMS oligomers and *n*-alkanes [19]. Once again the lower slope of the silicone curve compared to the hydrocarbon one can be seen, but more noticeable is the distinct difference in values: the interfacial tensions for PDMS are much lower than those for the *n*-alkanes, around 42.6 mN/m except for hexamethyldisiloxane, which is higher: at 44 mN m^{-1}. These significantly lower values can be attributed to the interaction of water molecules with the oxygen atoms in the siloxane bonds, facilitated by the pronounced flexibility of the siloxane backbone chain.

The literature also contains reports of a number of studies of interfacial tension between two different polymers (γ_{12}). Table 1.3 gives examples where PDMS was one of the components, taken from Kuo's compilation [20]. It can be seen that the temperature coefficients for interfacial tension are much lower than for surface tension, which results from the smaller density difference between two polymers compared to the individual polymer densities. Generally, the more polar the polymer, the larger is the interfacial tension with PDMS although there is no numerical equality between the interfacial tension and the difference of the two surface tensions (Antonow's rule [21]).

Note that in this table, for purposes of comparison, values are quoted at room temperature. As most polymers other than PDMS are solid at this temperature (melting point of PDMS is between −40 and −35 °C) the data presented are extrapo-

Table 1.3 Interfacial tension at 20 °C between various polymers and PDMS

Polymer	γ_{12} (mN m^{-1})	$-\delta\gamma/\delta T$ (mN {m K}$^{-1}$)
Polypropylene	3.2	0.002
Poly(*t*-butyl methacrylate)	3.6	0.003
Polyisobutylene	3.9	0.016
Polybutadiene	4.2	0.009
Poly(*n*-butyl methacrylate)	4.2	0.004
Polyethylene	5.3	0.002
Polystyrene	6.1	*ca* 0
Polytetrahydrofuran	6.3	0.0004
Polyoxytetramethylene	6.4	0.001
Polychloroprene	7.1	0.005
Poly(vinyl acetate)	7.4	0.008
Polyoxyethylene	9.9	0.008

lations from higher temperature studies so although the temperature coefficient is small, the data are not as absolute as might be imagined. Interfacial tension should change discontinuously at the crystal/melt transition and continuously at the glass transition with discontinuous $\delta\gamma/\delta T$. Wu [22] has shown that extrapolation is usually adequate as semi-crystalline polymers generally have amorphous surfaces when cooled from the melt.

1.3 Water Contact Angle Studies

The contact angle θ of a liquid on a solid is the angle between the liquid and the solid at the three-phase (liquid, solid, vapor) point of contact measured through the liquid phase (see also Chap. 5, Appendix A.3). The advancing angle θ_a is that for a liquid contacting a previously unwetted surface whereas the receding angle θ_r relates to a liquid that has already wetted the surface in question. Figure 1.3 illustrates this situation. If the drop is held stationary and the sample and stage moved to the left as shown, it is clear that the left hand side of the drop is in contact with previously wetted sample surface whereas the right hand side of the drop contacts unwetted surface.

The difference between the advancing and receding angles is called the contact angle hysteresis. Contact angle hysteresis is very common. Its diverse causes include surface roughness, chemical heterogeneity, surface reorganization, swelling, extraction of leachable species and chemical reaction. As a general rule, surfaces that exhibit little contact angle hysteresis are likely to be freer of these complications than more hysteretic surfaces.

There is a great variety of wetting studies of PDMS by water described in the literature which report a rather surprising broad range of advancing contact angles (θ_a) extending from 95° to 120°. These investigations deal with three broad classes

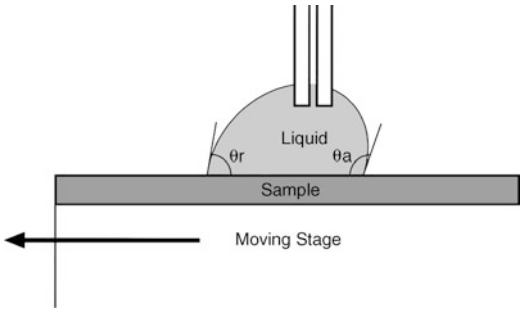

Fig. 1.3 Contact angle hysteresis. θ_r is the receding contact angle; θ_a is the advancing contact angle. Reprinted from Ref. [23] with kind permission of © The American Chemical Society (2003)

Table 1.4 Selected water contact angle data

Polymer cure	Authors	Contact angle method	θ_a (°)	θ_r (°)
Peroxide	Kennan et al. [27]	Sessile drop	111	57
Hydrosilylation	Kennan et al. [27]	Sessile drop	114	60
Peroxide	Kennan et al. [27]	Captive bubble	120	70
Hydrosilylation	Kennan et al. [27]	Captive bubble	122	73
Hydrosilylation	Wynne et al. [28]	Wilhelmy plate	118/108	83/87
End-grafted	She et al. [29]	Sessile drop	118	92
PHMS/PDMS	She et al. [29]	Sessile drop	108	105

of PDMS surfaces (a) PDMS fluids baked or otherwise adsorbed onto solids such as glass or metals, (b) cross-linked polymers on flexible substrates such as paper or plastic, and (c) PDMS elastomer surfaces. Given the propensity of PDMS to remain liquid to high molecular weights, these three classes essentially represent different strategies for immobilizing the surface sufficiently for contact angle study. One widely quoted value for the advancing contact angle of water on PDMS is 101° from the seminal studies of Zisman and co-workers [4]. It is an example of the first class of studies but is now regarded as a somewhat low value. Values in the 110° to 120° range are now considered more realistic—see Table 1.4. Gordon and Colquhoun's study [24] of PDMS release liners for pressure-sensitive adhesives and Chaudhury and Whitesides' [25] characterization of elastomeric PDMS are classic examples of the other two classes.

Part of the variation in results obtained surely derives from neglect of many pitfalls inherent to contact angle measurement. For example, using water of insufficient purity would lower its surface tension and result in reduction of the contact angle. The effect of surface roughness is to increase the contact angle which cautions against favoring the higher values as probably uncontaminated. Other drawbacks are unique to each class of measurement. For instance, when a PDMS film is adsorbed onto a rigid glass or metal substrate, the maximum hydrophobic effect is not initially evident and a thermal baking treatment is required to develop the familiar, high water repellency. This phenomenon was first documented by Hunter et al. [26] over 60 years ago but is still not fully understood. It could be that residual bound water is thermally removed during the baking allowing for more immobiliz-

ing siloxane/surface interactions but residual or surface-catalyzed creation of silanol groups on the polymer that can condense with surface hydroxyls or cross-link with each other are probably also involved. Hunter's initial water contact angles on films formed on glass by dipping in benzene solution were as low as 50° and heat treatment to 200 °C was required to obtain values in excess of 100°.

These difficulties are much less pronounced in the other two classes of measurement where adequate cross-linking is ensured but micro-roughness effects become more evident, both from fillers present in the underlying substrates and from the elastomer surface texture themselves. Morphological differences in coating surfaces resulting from how the coatings are formed (e.g. solvent cast, emulsion based or neat), are also a factor. Although not so important for water studies, the propensity of organic liquids to swell PDMS also plays a role. This is a particular problem with *n*-alkanes which are the preferred contact angle test liquids for determining the Zisman critical surface tension of wetting (γ_C) and other surface energy measurement approaches for low energy polymer surfaces.

There are surprises that arise even where care is taken to eliminate experimental artifacts. In a study by Kennan and co-workers [27] medical-grade silicone elastomers cross-linked in two different ways, by peroxide cure and by hydrosilylation cure, were subjected to accelerated aging in saline solution to verify the hydrolytic stability. Both advancing and receding contact angles of pure water were measured, using two different methods of measurement, the sessile drop method and the captive bubble method. These and other related data are shown in Table 1.4.

An even greater surprise emerges from a third method of measuring contact angle, the Wilhelmy plate approach. Wynne and co-workers [28] studied hydrosilylation cured PDMS coatings that are analogs of biomedical silicone materials. One type of PDMS was a commercial divinyl-terminated PDMS, while the other, a low polydispersity version, was synthesized in the laboratory. They found for both materials that an initial wetting/dewetting cycle of the Wilhelmy plate gave higher advancing contact angle and a lower receding contact angle than was the case for the second and subsequent wetting/dewetting cycles of the Wilhelmy plate. These data are also included in Table 1.4 as initial values/subsequent values. The authors [28] attributed this difference to contamination of the water by the PDMS sample although the nature of this contamination was not unambiguously identified. The presence of low molecular weight linear and cyclic oligomers is common in PDMS and a molecule like hexamethyldisiloxane could certainly be leached out into the aqueous phase. However, in many studies including the Kennan data (Table 1.4), the materials studied have been rigorously extracted and unlikely to be contaminated in this manner. Furthermore, contamination is not the only conceivable explanation. It is also possible that the siloxane backbone becomes hydrated on contact with water and that the higher advancing contact angle is that of the unhydrated state and the lower value corresponds to the hydrated situation.

She et al. [29] attempted to create a PDMS surface that did not suffer from the drawbacks of the three classes of studies described above. Working from the premise that what is required is a very thin film of un-filled PDMS attached by a well-understood, low-temperature chemistry to a very smooth, rigid substrate, they

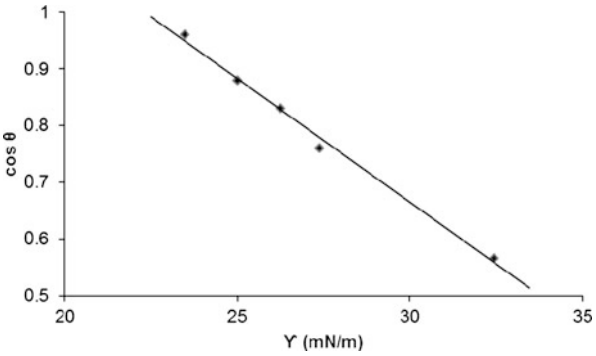

Fig. 1.4 Zisman plot of PDMS. Reprinted from Ref. [29] with kind permission of © The American Chemical Society (2000)

began with carefully cleaned silicon wafers that had been lightly plasma-oxidized to produce a thin silanol-functional, silica layer. A self-assembled monolayer of undecenyltrichlorosilane ($Cl_3Si(CH_2)_9CH{=}CH_2$) was then formed on this surface and SiH-functional PDMS polymers grafted onto this surface by platinum catalyzed hydrosilylation. Two types of polymer were used, monofunctional linear polymers of varying chain length, and a polydimethylsiloxane/polymethylhydrogensiloxane (PDMS/PHMS) copolymer ($Me_3Si(OMe_2Si)_{145}(OSiMeH)_{20}OSiMe_3$). Any unreacted polymer chains were removed by solvent extraction. The data of She et al. for the longest grafted chain and the copolymer are also shown in Table 1.4. Note how little contact angle hysteresis is exhibited by these two surfaces.

1.4 Solid Surface Energy Determination

The oldest approach to quantifying solid polymer surface energies is that of Zisman and co-workers [4]. They found that when the cosines of the contact angles of a series of liquids placed on the solid are plotted against their surface tensions, an almost linear plot is obtained. A PDMS example is shown in Fig. 1.4. The extrapolation of this line to $\cos\theta = 1$, i.e. zero contact angle, is known as the critical surface tension of wetting of that solid. It is the surface tension of the hypothetical liquid that just wets the polymer and as such has correctly, and perhaps pedantically, units of mN/m rather than mJ/m^2. Note that it is not equal to the solid surface free energy because it ignores the possible interfacial tension between the liquid and the solid. Using this approach Shafrin and Zisman [29] developed the order of the impact of substituent groups in polymers on surface energy referred to in Sections 1.1 and 1.2. Critical surface tension of wetting values, γ_C, from Shafrin and Zisman and She et al. for PDMS are shown in Table 1.5.

Surface and interfacial energies are related to the contact angle by the Young equation:

$$\gamma_{SV} - \gamma_{SL} = \gamma_{LV}\cos\theta \tag{1.2}$$

where the subscripts SV, LV, and SL refer to the solid/vapor and liquid/vapor surfaces, and the solid/liquid interface, respectively. Obviously, to use this equation to

Table 1.5 A summary of solid surface energy data for PDMS

Quantity	Authors	Value
γ_C (mN m^{-1})	Shafrin and Zisman [30]	24
γ_C (mN m^{-1})	She et al. [29]	22.7
γ_{JKR} (mJ m^{-2})	Chaudhury [15]	22.6
γ_{SV} ($\gamma_{SV}^d + \gamma_{SV}^p$) (mJ m^{-2})	Owens and Wendt [33]	22.8 (21.7 + 1.1)
γ_{SV}^d (mJ m^{-2})	She et al. [29]	21.3

derive surface energies, liquids that form a finite contact angle and do not spread on the substrate must be selected. This equation was first described in 1805 but was not experimentally verified until 1971 when Johnson, Kendall and Roberts [14] introduced their contact mechanics approach to surface and interfacial energies independent of contact angle measurement. The Young equation can be combined with the Dupré equation for W_{SL}, the thermodynamic work of adhesion of a liquid to a solid:

$$W_{SL} = \gamma_{SV} + \gamma_{LV} - \gamma_{SL} \tag{1.3}$$

Combining Eqs. (1.2) and (1.3) gives

$$W_{SL} = \gamma_{LV}(1 + \cos\theta) \tag{1.4}$$

Girifalco and Good [31] proposed that W_{SL} could be expressed in a geometric mean form of the surface energies of the liquid and solid phases as

$$W_{SL} = 2\Phi\,(\gamma_{SV}\gamma_{LV})^{0.5} \tag{1.5}$$

where Φ is a correction factor for intermolecular interactions that equals unity if the intermolecular forces acting across the interface are alike. This is a reasonable approximation for n-alkanes on the predominantly non-polar PDMS surface, so it follows that by combining these equations with $\Phi = 1$ one obtains

$$\gamma_{SV} = \gamma_{LV}(1 + \cos\theta)^2/4 \tag{1.6}$$

also known as the Girifalco, Good, Fowkes, Young (GGFY) equation. It provides a useful way of estimating surface energy, or at least the dispersion force component, of apolar polymers from their contact with one liquid, usually n-hexadecane as it is the highest surface tension n-alkane at room temperature. This equation, using the data of She et al. [29], gives a value of 21.3 mJ/m^2 for PDMS (see Table 1.5).

Fowkes [32] suggested that the surface energy of a solid is made up additively of components that correspond to intermolecular interactions. As many as seven terms have been suggested but a common simplification is to consider only two: the component resultant from electrodynamic London dispersion forces common to all matter, known as the dispersion force component (γ_{SV}^d), and the so-called polar component (γ_{SV}^p) that incorporates all other interfacial interactions. One of the most frequently used two-component methods is that of Owens and Wendt [33] shown in Eq. (1.7):

$$\gamma_{LV}(1 + \cos\theta) = 2\left(\gamma_{LV}^d\gamma_{SV}^d\right)^{0.5} + 2\left(\gamma_{LV}^p\gamma_{SV}^p\right)^{0.5} \tag{1.7}$$

The two unknowns, γ^d and γ^p, of the solid require two contact angle liquids. Water and methylene iodide (diiodomethane) are a common choice, the former being predominantly polar and the latter primarily nonpolar, with both liquids having a high surface tension conducive to forming finite contact angles on a given solid. There are sound reasons to suppose that dispersion forces interact in a geometric mean fashion but this is certainly not so for polar interactions so this approach is only semi-empirical. PDMS data from Owens and Wendt are included in Table 1.5.

Also included in Table 1.5 is a JKR contact mechanics value that is further discussed in the next section. Table 1.5 is a very limited, personal selection from a much greater body of data, however, the relative closeness of these values obtained in very different ways is comforting but perhaps illusory.

1.5 Contact Mechanics Approach

Contact mechanics, as the name implies, is concerned with the behavior of solids in contact under the action of an external load. From the perspective of silicone surface science, the great interest in this topic in recent decades is driven by the realization that it offers an alternative way of measuring surface energies free from the vagaries inherent in contact angle approaches. Hertz in 1882 was the first to address this topic. However, he took no account of interfacial interactions considering only frictionless, non-adhering surfaces of perfectly elastic solids. This neglect is more obvious for relatively small particles contacting each other on a flat surface when it is evident that contact deformations are larger than those predicted by the Hertz theory.

Johnson, Kendall and Roberts [14] reasoned that these excess deformations were the result of attractive forces. They assumed that the attractive forces were confined within the area of contact and used an energy balance approach to develop a general expression for the contact deformation as a function of the surface and elastic properties of solids, now widely known as the JKR theory. However, this theory is not the only one accounting for contact between solids. The so-called DMT theory introduced by Derjaguin et al. [34] assumes that all the attractive forces lie outside the area of contact which is under compression as described by the Hertzian strain profile and makes significantly different predictions from those of the JKR theory. As a consequence, there has been considerable discussion in the literature concerning the relative merits of these two theories which have since been shown to describe different limiting cases of a more general situation. There is now general agreement that the DMT approach is most suitable for hard, low-surface-energy materials with small radii of curvature, whereas the JKR approach is most suited to soft materials with relatively high surface energies and large radii of curvature. In practice, it transpires that the JKR theory correctly accounts for the contact behavior of soft polymeric materials, including low-surface-energy silicones, and it is, therefore, the only approach that is considered in this chapter.

The application of the JKR approach to silicone surfaces was pioneered by Chaudhury and Whitesides [15, 25]. As pointed out by them, PDMS is an ideal

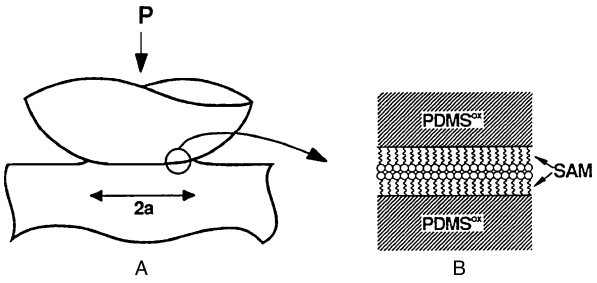

Fig. 1.5 Contact between a semi-spherical lens and flat sheet of PDMS. Both surfaces have been modified with an alkoxysilane self-assembled monolayer (SAM)

substrate for such studies. The surface of the deformable component must be very smooth and homogeneous and this has been shown to be the case for PDMS by electron microscopy. No structural inhomogeneity is evident even at a resolution of 20–30 nm. Of course, it must be possible to cast the material into spherical or semi-spherical shapes and this is readily achieved with liquid, cross-linkable silicone formulations by forming drops on an ultra-low energy surface such as a fluorinated self-assembled monolayer (SAM) prior to cross-linking of the PDMS network A further advantage of PDMS substrates is that by plasma oxidation of the surface followed by SAM modification, the surface properties can be varied without affecting bulk physical properties.

The original approach of Chaudhury and his co-workers was to bring a semi-spherical lens and a flat sheet of PDMS into contact and measure the resulting contact deformation under controlled loads. This was then extended to other flat surfaces, notably silicon wafers modified by a variety of self-assembled monolayers [35]. They have also extended the sample geometry to a cylinder rather than a sphere [36] and used rolling contact mechanics to study adhesion hysteresis at the interface of plasma-oxidized PDMS elastomer rolling on a PDMS film grafted to a silicon wafer. It should be also noted that other geometries are amenable to JKR analysis and that Chaudhury's group is not the only one using the JKR approach to investigate polymer surfaces. The surface forces apparatus (SFA) originally developed by Tabor and Winterton [37] is used in this way. In this apparatus thin polymer film samples coated onto molecularly smooth thin mica sheets, often in a crossed cylinder configuration, are brought into contact. Tirrell and co-workers [38, 39] in particular have used the SFA to characterize a variety of polymer substrates.

When a deformable semi-spherical solid with radius of curvature R and a flat plate are brought into contact the result is the formation of a circular region of contact of radius "a" whose size depends on the surface forces and the external applied load P. A diagram of this geometry is shown as A in Fig. 1.5. The enlargement of the interfacial contact area shown as B in Fig. 1.5 illustrates how the surfaces may be modified by a self-assembled monolayer (SAM). The $PDMS^{OX}$ layer is a thin silica-like layer produced by plasma oxidation of the PDMS surface [35].

For this sphere on plate geometry, Johnson, Kendall and Roberts [14] showed that

$$a^{3/2}/R = (1/K) \cdot \left(P/a^{3/2}\right) + (6\pi \mathrm{W}/\mathrm{K})^{1/2} \tag{1.8}$$

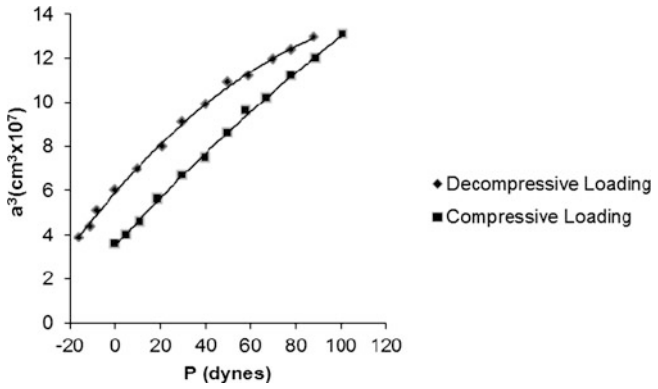

Fig. 1.6 JKR plot for PDMS against a fluoroalkylsiloxane monolayer. Reprinted from Ref. [40] with kind permission of © The American Chemical Society (1993)

Table 1.6 Comparison of surface energies derived from JKR and contact angle data [35]

Silane SAM head-group	γ_{JKR} (mJ m^{-2})	γ_{SV}^{d} (mJ m^{-2})	γ_{SV}^{p} (mJ m^{-2})	γ_{SV} (mJ m^{-2})
$-CF_3$	16.0	15.0	0.8	15.8
$-CH_3$	20.8	20.6	0.1	20.7
$-OCH_3$	26.8	30.8	6.4	37.2
$-CO_2CH_3$	33.0	36.0	6.4	42.4
–Br	36.8	37.9	1.7	39.6
Polyethylene	33	32.0	1.1	33.1

where K is the composite elastic modulus and W is the thermodynamic work of adhesion. Since for two identical surfaces W is simply $2\gamma_{SV}$, the solid surface energy, γ_{JKR}, can be derived by contacting two of the same surfaces. A typical plot of the applied load P against $a^{3/2}$ for PDMS against a fluoroalkylsiloxane monolayer is shown in Fig. 1.6. The curves follow different paths as the applied load is increased or decreased thus showing hysteresis in a similar manner as do advancing or receding contact angles. Because of the action of the attractive forces across the interface, a finite tensile force is required to separate the surfaces from adhesive contact. Johnson, Kendall and Roberts showed that this "pull-off" force, P_S, is given by

$$P_S = 3\pi W R/2 \tag{1.9}$$

Chaudhury's [15] value of 22.6 mJ m^{-2} for γ_{JKR} of PDMS is given in Table 1.5. Table 1.6 lists his results from a study of the surface free energy of alkylsiloxane monolayers supported on elastomeric PDMS [35] as shown in B of Fig. 1.5. The value for polyethylene is also included so that it can be seen that the surface energy follows the order first described by Zisman and co-workers, $CF_3- <$

Table 1.7 Selected values of JKR interfacial tension between various polymers and PDMS [38]

Polymer	γ_{12} (mN m^{-1})
Poly(vinyl cyclohexane)	3
Poly *p*-*t*-butylstyrene	9
Polystyrene	10
Poly *p*-phenylstyrene	11
Poly(vinyl benzyl chloride)	12
Polyacrylonitrile	20

CH_3- < $-CH_2-$, but note that a γ_{JKR} value for $-CF_2-$ has not been reported yet to the best of our knowledge. Contact angle values of γ_{SV} derived using Eq. (1.7) with water and methylene iodide (except for the $-CF_3$ surface where perfluorodecalin was used instead of methylene iodide) are included in Table 1.6 for comparison. Agreement is quite close for the non-polar substrates but not so good for the polar entities.

The literature also contains reports on some polymer interfacial tension studies involving PDMS determined by the JKR contact mechanics approach. Some pertinent data are shown in Table 1.7 [38]. It can be seen that only one polymer pair, PDMS/polystyrene, replicates any data listed in Table 1.3. However, the JKR solid/solid interfacial energy value of 10 mJ m^{-2} is quite different from the melt extrapolation value of 6.1 mN m^{-1} in Table 1.3. Coincidence of these two different quantities is not to be expected. As with the melt studies, there is a trend for higher surface energy, more-polar polymers to have a higher interfacial energy with PDMS.

1.6 Langmuir Trough Studies

Being of low surface-energy and insoluble in water but also having a polar backbone to interact with the water surface, PDMS and some other silicone polymers are able to spread over water surfaces thus making it possible to study the behavior of their surface pressure/surface area isotherms by the Langmuir trough technique. An example of such behavior is given in Fig. 1.7 [41]. From this figure it can be seen that the isotherm has essentially four regions; an initial low surface-pressure region (A_1–A_2) followed by a rise in surface pressure (A_2–B) which leads to a plateau region (B–C) followed by a final small rise and a very small plateau before reaching the collapse point. Chapter 7 of this book covers Langmuir trough behavior of silicones but the subject is briefly reviewed here for the sake of completeness.

There has been much varied interpretation of these PDMS isotherms over the years. For a long time a model introduced by Fox et al. [42] was accepted, according to which at low surface-pressure every siloxane bond was envisioned in contact

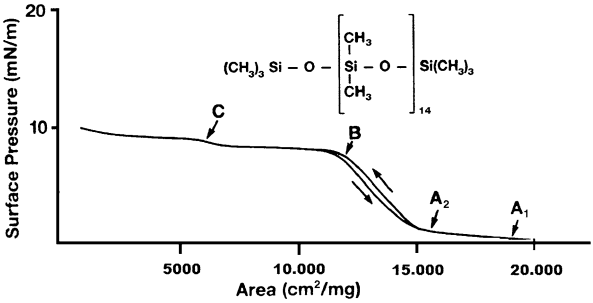

Fig. 1.7 Langmuir trough isotherm for PDMS. This material is reproduced from Ref. [41] with kind permission of © John Wiley & Sons, Inc. (1971)

with the water surface and all the methyl groups were assumed to be oriented outwards towards the air phase. At higher surface pressures the spread monolayer was supposed to transition to a six-unit helical coil whose axis is parallel to the water surface. The considerable reduction in surface area caused by this transition was used to explain the characteristic plateau in the PDMS isotherm in the 8–10 mN m^{-1} surface pressure region. More than a decade later, Noll and co-workers [41] suggested a modification of this model involving hydration of the polymer backbone and squeezing out of the water molecules as the film is compressed in the low-surface-pressure region.

In 1989, Granick and co-workers [43] questioned the helical coiling concept when they found that cyclic PDMS with as few as 20 monomer units also showed this plateau. Later Mann et al. [44] challenged the implied homogeneous monolayer assumption of the original model by demonstrating the co-existence of domains of different surface density at very low surface-pressures using Brewster angle microscopy. Most recently Kim et al. [45] applied the sum frequency generation technique (see Chap. 2) to this problem and concluded that in the initial low-surface-pressure region the methyl groups do not all point outwards to the air phase. Their results indicated either a totally random orientation of the methyl groups or one where one of the methyl groups is pointing directly out and the other is pointing inwards to the water. The first of these possibilities would seem to be the most likely. Neutron reflectivity studies suggest a PDMS layer thickness of *ca.* 15 Å in the dilute region, twice that of a single spread monolayer, consistent with a disordered, freely rotating chain concept. The rising surface pressure region up to the plateau seems to involve PDMS chains lying at the interface with both methyl groups pointing towards the air with one closer normal to the surface and the other closer to the interface. The results for the plateau region are more consistent with a horizontal chain folding geometry than with contraction into helices. The horizontal chain folding idea was first proposed by Kalachev et al. [46] based on surface potential studies.

At present, we doubt that we have heard the last of explanations of Langmuir trough behavior of PDMS and related polymers. The technique has been applied to a variety of other silicones including, cyclo-linear polysiloxanes [47] where up to seven plateaus were observed, polar-group substituted siloxanes such as amino and quaternary ammonium functional polymers [48], and poly(amidoamine-organosilicon) dendrimers [49].

Table 1.8 Surface tension of polysiloxanes other than PDMS

Polymer	Viscosity (cS)	Surface tension ($mN\,m^{-1}$)
Polymethylphenylsiloxane [50]	500	28.5
Polydiethylsiloxane [51]	Unknown	25.7
Polymethyltrifluoropropylsiloxane [18]	Infinite	24.4
Polymethylhydrogensiloxane [52]	30	20
Polydimethylsiloxane [18]	Infinite	20.9

Table 1.9 Surface energies of selected fluoropolymers

Polymer	γ_C ($mN\,m^{-1}$)	γ_{SV} ($mJ\,m^{-2}$)	γ_∞ ($mN\,m^{-1}$)
Polydimethylsiloxane	22.7	22.8	21.3
Polymethyltrifluoropropylsiloxane	21.4	13.6	24.4
Polymethylnonafluorohexylsiloxane	16.3	9.5	19.2
Polytetrafluoroethylene	18.5	14.0	25.9
Polyhexafluoropropylene	16.2	12.4	–
Polyoxyhexafluoropropylene	–	–	18.4

1.7 Other Silicones

Although they are extensively used in surface modification, very little systematic information has been reported concerning the surface energy of silicone polymers with functional entities in the pendant side-groups. A major reason for this is that silicones with polar functionalities such as aminofunctional PDMS incorporate the polar entity to enhance substantivity to substrates while maintaining PDMS surface properties. Consequently, they are usually copolymers with PDMS whose surface energy behavior is dominated by the PDMS component.

Even among the silicone homopolymers other than PDMS there is a paucity of reported surface energy data in the literature. Some liquid surface tension values are available and a selection of such data for the commercially more important homopolymers is given in Table 1.8. No temperature dependence data have been reported and in most cases insufficient data are available to extrapolate to infinite molecular weight as can usefully be done for PDMS. Not surprisingly, however, the exception to this is the fluorosilicones as they offer the only prospect of improving on the already considerable low surface energy of PDMS (see Table 1.9, Chap. 5).

The polymethylphenylsiloxane has an expectedly higher surface tension than PDMS because of the aromatic ring current. Polydiethylsiloxane is included in this list because of growing interest in the West. It has long been a favorite silicone in Russia but only recently has much attention been paid to it in Europe and the USA. The higher PMTFPS value than that for PDMS is briefly discussed in Section 1.2. The polymethylhydrogensiloxane measurement was made at 37 °C. A similar viscosity PDMS at this temperature would have a very comparable liquid surface

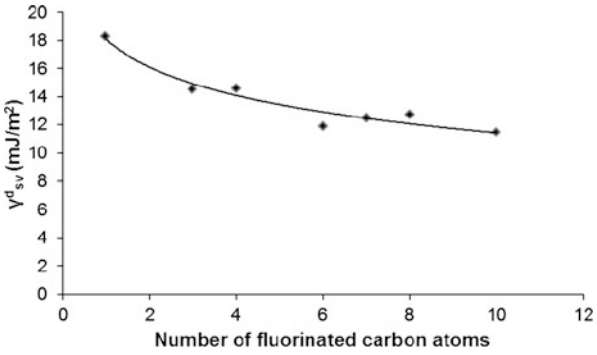

Fig. 1.8 Dispersion force component of surface energy versus fluorinated side-chain length for fluorosilicones

tension of 20.5 mN m^{-1}, implying that the SiH entity has a similar intrinsic surface energy to CH_3.

Table 1.9 summarizes the more complete surface property data available [18] for PMTFPS and polymethylnonafluorohexylsiloxane (PMNFHS). Also included for comparative purposes are polytetrafluoroethylene (PTFE), polyhexafluoropropylene (PHFP) and polyoxyhexafluoropropylene (POHFP). Critical surface tensions were all determined using *n*-alkanes and the solid surface tensions were obtained by the Owens/Wendt approach [33] using water and methylene iodide so data in each column can be usefully compared. Note that with PMNFHS a fluorosilicone is available that has a lower surface energy than PDMS in all three of these surface properties.

Figure 1.8 presents some further data on silicone polymers of the same structure as PMTFPS, that is to say, those that retain one methyl group on every silicon atom. This structure has process benefits in that it expands the range of possible solvents and also encourages chain extension over formation of cyclics but it does hinder the attainment of very low surface energies. These data are from the work of Doeff and Lindner [53] and one of us [54] using Eq. (1.6) with *n*-hexadecane as the contact angle liquid. The figure shows the feature that is typical for all fluoropolymers, namely a decrease in surface energy with the lengthening of the fluoroalkyl pendant group. This is usually explained as a consequence of burying the transient dipole that occurs at the fluorocarbon/hydrocarbon chain junction. The fluorocarbon groups also polarize the adjacent $–CH_2–$ groups making them rather acidic which may also be the explanation. It is not completely clear why the effect persists to quite a depth, *ca.* six fluorinated atoms being required before the plateau of 11–12 mJ m^{-2} is reached. However, this does suggest that there would be little advantage in pursuing longer fluorocarbon side-chains, particularly with the bio-accumulation concerns of such entities. Note also that Thanawala and Chaudhury [55] have reported a surface energy of 7.5 mJ m^{-2} for a $F[CF(CF_3)CF_2O]_7CF(CF_3)CONHCH{=}CH_2$ modified PDMS surface also using *n*-hexadecane and the GGFY equation. The lowest surface energies for fluorosilicones are found with the fluorocarbon-substituted polyhedral oligomeric silsesquioxanes which contain no methyl groups. These are the subject of Chapter 6; other fluorosilicone polymers are reviewed in Chapter 5.

1.8 Concluding Remarks

Silicones, particularly PDMS, are widely exploited for their surface properties and behavior. In this chapter we have sought to establish the structure/property relationships of silicone surface science in order to set the stage for the elaboration of important topics pertaining to this field and comprising the contents of the following chapters.

The central position of PDMS in the silicone industry is a consequence of its structure. The combination of small methyl side-groups arrayed along the uniquely flexible siloxane backbone and exhibiting low inter-segmental attractive forces results in a polymer whose low surface energy can be equaled or bettered by relatively few other polymers. Moreover, it has the added bonus of greater thermal and oxidative stability than most comparable organic polymers. Smaller, pendant entities than the methyl group are not forthcoming. Likely atoms such as hydrogen or fluorine are reactive when directly linked to the silicon atom. Larger groups would dilute the special qualities such as extreme chain flexibility that the siloxane backbone confers. As a consequence, PDMS is used for its special surface properties in a wide variety of applications, some important examples of which are further considered in the final chapter of this book. The principal drawbacks of PDMS in this arena are its susceptibility to cleavage of the siloxane bond at extremes of pH and its oleophilicity. The former is shared by all polymers that have different alternating atoms in their backbone, while the solution to oleophilicity-causing difficulties is to turn to the more solvent-resistant fluorosilicones.

Nearly 20 years ago one of us [56] was bold enough to make a variety of predictions concerning silicone surface science and technology. Some of these predictions materialized but one in particular has failed so far to do so: the anticipated exploitation of more flexible backbones and new low-surface-energy pendant groups. Both polyphosphazenes and fluoroethers have expanded their scope but no new polymer backbone with significant greater flexibility than the siloxane chain has appeared. Nor has a lower surface energy substituent based on anything other than aliphatic fluorocarbon been found. Maybe current work with the SF_5–moiety might change this circumstance [57].

References

1. Warrick EL (1990) Forty years of firsts. McGraw-Hill, New York
2. Mark JE (1978) Macromolecules 11:627
3. Langmuir I (1916) J Am Chem Soc 38:2221
4. Zisman WA (1964) In: Fowkes FM (ed) Contact angle, wettability and adhesion. Adv Chem Ser, vol 43. Amer Chem Soc, Washington, p 1
5. Shih H, Flory PJ (1972) Macromolecules 5:758
6. Owen MJ (2000) Surface properties and applications. In: Jones RG, Ando W, Chojnowski J (eds) Silicon-containing polymers. Kluwer, Dordrecht, pp 213–231
7. Kurian P, Kennedy JP, Kisliuk A, Sokolov A (2002) J Polym Sci, Part A, Polym Chem Ed 40:1285

8. Dvornic PR (2000) Thermal properties of polysiloxanes. In: Jones RG, Ando W, Chojnowski J (eds) Silicon containing polymers. Kluwer, Dordrecht, pp 185–212
9. Schiers J (1997) Perfluoroethers: synthesis, characterization and applications. In: Schiers J (ed) Modern fluoropolymers. Wiley, New York, pp 435–485
10. Lee WA, Rutherford RA (1975) In: Brandrup J, Immergut EH (eds) Polymer handbook, 2nd ed. Wiley, New York, pp 111–139
11. Kobayashi H, Owen MJ (1990) Macromolecules 23:4929
12. Nielson RH, Hani R, Wisian-Nielson P, Meister JJ, Roy AK, Hagnauer JL (1987) Macromolecules 20:910
13. Dvornic PR, Jovanovic JD, Govedarica MN (1993) J Appl Polym Sci 45:1497
14. Johnson KL, Kendall K, Roberts AD (1971) Proc R Soc London A 324:301
15. Chaudhury MK, Whitesides GM (1991) Langmuir 7:1013
16. Owen MJ (1980) Ind Eng Chem Prod Res Dev 19:97
17. LeGrand DG, Gaines GL (1969) J Colloid Interface Sci 31:162
18. Falsafi A, Mangipudi S, Owen MJ (2006) Surface and interfacial properties. In: Mark JE (ed) Physical properties of polymers handbook 2nd ed. Am Inst Phys, New York. Chap 59
19. Kanellopoulos AG, Owen MJ (1971) Trans Faraday Soc 67:3127
20. Kuo ACM (1999) Polydimethylsiloxane. In: Mark JE (ed) Polymer data handbook. OUP, New York, pp 411–435
21. Antonow GN (1907) J Chim Phys 5:372
22. Wu S (1982) Polymer interface and adhesion. Dekker, New York
23. Owen MJ (2003) Surface energy. In: Brady RF (ed) Comprehensive desk reference of polymer characterization and analysis. Am Chem Soc, New York. Chap 15
24. Gordon DJ, Colquhoun JA (1976) Adhes Age 19(6):21
25. Chaudhury MK, Whitesides GM (1992) Science 255:1231
26. Hunter MJ, Gordon MS, Barry AJ, Hyde JF, Heidenreich RD (1947) Ind Eng Chem 39:1389
27. Kennan JJ, Peters YA, Swarthout DE, Owen MJ, Namkamisorn A, Chaudhury MK (1997) J Biomed Mater Res 36:487
28. Wynne KJ, Lambert JM (2004) Silicones. In: Encyclopedia of biomaterial and biomedical engineering. Dekker, New York, pp 1348–1362
29. She H, Chaudhury MK, Owen MJ (2000) In: Clarson SJ, Fitzgerald JJ, Owen MJ, Smith SD (eds) ACS Symp Ser, vol 729, pp 322–331
30. Shafrin EG, Zisman WA (1960) J Phys Chem 64:519
31. Good RJ, Girifalco LA (1960) J Phys Chem 64:561
32. Fowkes FM (1964) Ind Eng Chem 56:40
33. Owens DK, Wendt RC (1969) J Appl Polym Sci 13:1741
34. Derjaguin BV, Muller VM, Toporov YP (1975) J Colloid Interface Sci 53:314
35. Chaudhury MK (1993) J Adhes Sci Technol 7:669
36. She H, Malotky D, Chaudhury MK (1998) Langmuir 14:3090
37. Tabor D, Winterton RHS (1969) Proc R Soc London Ser A 312:435
38. Mangipudi VS, Tirrell M, Pocius AV (1995) Langmuir 11:19
39. Li L, Mangipudi VS, Tirrell M, Pocius AV (2001) In: NATO Science Series II, Mathematics, Physics and Chemistry, vol 10, pp 305–329
40. Chaudhury MK, Owen MJ (1993) Langmuir 9:29
41. Noll W, Steinbach H, Sucker C (1971) J Polym Sci, Part C 34:123
42. Fox HW, Taylor PW, Zisman WA (1947) Ind Eng Chem 39:1401
43. Granick S, Kuzmenka DJ, Clarson SJ, Semlyen JA (1989) Macromolecules 22:1878
44. Mann EK, Henon S, Langevin D, Meunier J (1992) J Phys II (France) 2:1683
45. Kim C, Gurau MC, Cremer PS, Yu H (2008) Langmuir 24:10155
46. Kalachev AA, Litvinov VM, Wegner G (1991) Makromol Chem, Macromol Symp 46:365
47. Fang J, Dennin M, Knobler CM, Godovsky YK, Makarova NN, Yokoyama H (1997) J Phys Chem B 101:3147
48. Mehta SC, Somasundaran P, Maldarelli C, Kulkarni R (2006) Langmuir 22:9566
49. Dvornic PR, De Leuze-Jallouli A, Perz SV, Owen MJ (2000) Mol Cryst Liq Cryst 353:223

50. http://www.clearcoproducts.com. Accessed 23 March 2011
51. http://www.accudynetest.com. Accessed 23 March 2011
52. Schurch S, Georke J, Clements JA (1976) Proc Natl Acad Sci USA 73:4698
53. Doeff M, Lindner E (1989) Macromolecules 22:2951
54. Kobayashi H, Owen MJ (1995) Trends Polym Sci 3:330
55. Thanawala SK, Chaudhury MK (2000) Langmuir 16:1256
56. Owen MJ (1993) Surface chemistry and applications. In: Clarson SJ, Semlyen JA (eds) Siloxane polymers. Prentice Hall, New York, pp 309–372
57. Kostov G, Ameduri B, Sergeeva T, Dolbier WR Jr., Winter R, Gard GL (2005) Macromolecules 38:8316

Chapter 2
Sum Frequency Generation Vibrational Spectroscopy of Silicone Surfaces & Interfaces

Dongchan Ahn and Ali Dhinojwala

2.1 Introduction

Silicone materials such as polydimethylsiloxane (PDMS) exhibit very unusual surface properties that arise from the unique flexibility, bond energy, partially ionic nature of the siloxane (Si-O) backbone, and low intermolecular forces [1, 2]. These molecular features are manifested in bulk properties such as low surface energy, heat stability, low temperature flexibility, dielectric strength, inertness, hydrophobicity, optical clarity and ease of crosslinking by a variety of mechanisms that have allowed silicones to grow from a research concept in the early 20th century to a virtually ubiquitous material set used in a remarkably diverse variety of industries and applications [3]. For example, Dow Corning Corporation, which was established in 1943, has grown to a $6 billion company in 2010, based largely on silicones going into over 6,000 products spanning nearly every major commercial industry. In particular, the unique range of surface and interfacial properties attainable in a facile manner through the versatility of organosilicon chemistry positions silicones well for even greater future prominence as products and processes leverage structural control over ever-diminishing length scales.

Paramount to the effective development of micro- or nano-engineered materials are the structural and compositional insights from characterization of the interfaces. Despite remarkable advances in surface analysis techniques, elucidating direct structural information from interfaces remains difficult for a variety of reasons. Perhaps the most common challenge in surface science is the scarcity of the interface relative to large background signals from the 'bulk' that tend to result in poor sensitivity. Sum-frequency generation vibrational (SFG) spectroscopy offers

D. Ahn (✉)
Dow Corning Corporation, Midland, MI 48686, USA
e-mail: d.ahn@dowcorning.com

A. Dhinojwala (✉)
Department of Polymer Science, The University of Akron, Akron, OH 44325, USA
e-mail: ali4@uakron.edu

M.J. Owen, P.R. Dvornic (eds.), *Silicone Surface Science*, Advances in Silicon Science 4,
DOI 10.1007/978-94-007-3876-8_2,

intrinsic advantages in this regard, because the output is based on nonlinear optical selection rules that render it sensitive only to regions of a material where inversion symmetry is broken. In the majority of materials that are isotropic and homogeneous in the bulk, the technique is ideal for studying surfaces and buried interfaces non-invasively. The resulting output is an infrared (IR) vibrational spectrum that offers the same richness of molecular information and bonding with nearly unparalleled surface sensitivity.

While several general reviews of the applications of SFG appear in the literature, none have focused specifically on the application of SFG to silicones [4–10]. The reader is directed to these cited references for additional background and details on the technique and its use with other classes of materials. The unique and somewhat dichotomous surface properties of silicones, and their ever-increasing use in surface and interface-dependent applications such as lubricants, adhesives, microfluidic materials, sensors and matrices or scaffolds for nanocomposites, calls for increased fundamental understanding that has motivated the use of SFG analysis. The intent of this chapter is to focus specifically on the combination of this uniquely surface sensitive tool to study applications using PDMS and other silicone-based materials. We distinguish silicones from silicates and silanes by focusing on materials that have a flexible polymeric -Si-O-Si- backbone. For example, the body of references on SFG characterization of silane-based self-assembled monolayers or modified silica surfaces falls outside the scope of this review. We briefly overview the technique, then illustrate its utility in studying a number of important interfacial phenomena involving silicone-based materials by way of examples from the literature. Because the interpretation of SFG spectra can be quite complex, many of these examples highlight how SFG can be coupled with complementary techniques to provide a more complete understanding of interfacial effects. Lastly, we conclude by providing a summary of strengths, limitations and potential future opportunities for application of SFG and complementary techniques to silicone-based materials.

2.2 Fundamentals

2.2.1 Theory of Surface-Sensitive SFG

The theory of SFG has been explained in published works [11–14] and is not presented here at the same level of detail. The following background is sufficient for enabling the reader not familiar with SFG to understand the examples and case studies presented in the text [15].

When light interacts with a medium the polarization is expressed using the electric-dipole approximation as follows:

$$\mathbf{P} = \varepsilon_0(\chi^{(1)}:\mathbf{E} + \chi^{(2)}:\mathbf{EE} + \cdots) \tag{2.1}$$

Here, $\mathbf{P}$ is the polarization vector, $\mathbf{E}$ is the electric field vector, and $\boldsymbol{\chi}^{(1)}$ and $\boldsymbol{\chi}^{(2)}$ are the first- and second-order electric susceptibility tensors of the medium (higher-order susceptibilities are not shown and are usually negligible in magnitude). Also,

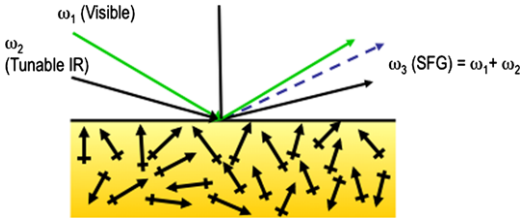

Fig. 2.1 Schematic diagram (not to scale) of a copropagating, external-reflection (ER) geometry used for SFG. The beams of frequencies ω_i are as follows: $i = 1$, S- or P-polarized visible; 2, S- or P-polarized IR; and 3, SFG. The SFG signal is detected after passing through a polarizer and filters

it is assumed that the medium does not have a permanent polarization (true for most organic materials). The second- and higher-order terms in the polarization equation are experimentally observed only when the medium is subjected to high electric field using a high intensity pulsed lasers. In infrared-visible SFG experiments, the medium is simultaneously subjected to two intense electric fields; then the induced polarization is as follows:

$$\mathbf{P} = \varepsilon_0\left(\boldsymbol{\chi}^{(1)}:(\mathbf{E}_1 + \mathbf{E}_2) + \boldsymbol{\chi}^{(2)}:(\mathbf{E}_1\mathbf{E}_2 + \mathbf{E}_2\mathbf{E}_1) + \cdots\right) \tag{2.2}$$

The meaning of $\mathbf{P}$, $\mathbf{E}_i$, and, $\boldsymbol{\chi}^{(j)}$ are the same as, or analogous to, those in (2.1).

When the source of electric fields is laser light as in Fig. 2.1, $\mathbf{E}_1 = \mathbf{E}_1^0\cos(\omega_1 t)$ and $\mathbf{E}_2 = \mathbf{E}_2^0\cos(\omega_2 t)$; therefore, it is easily seen with a trivial trigonometric rearrangement that the term containing $\boldsymbol{\chi}^{(2)}$ in (2.2) will have a sinusoidal component of frequency $\omega_1 + \omega_2$ which shows that $\boldsymbol{\chi}^{(2)}$ is responsible for SFG. The $\boldsymbol{\chi}^{(1)}$ term is responsible for linear optical-processes such as Raleigh and Raman scattering; however, unlike such scattering, the nonlinear SFG generates a coherent signal in the form of a collimated beam in a predictable direction. From symmetry arguments it can be shown that the third-rank tensor, $\boldsymbol{\chi}^{(2)}$, has a value of 0 in centrosymmetric media if it can be assumed that only electric-dipole mechanisms are responsible for $\boldsymbol{\chi}^{(2)}$, and the contributions from higher-order multipoles and magnetic dipoles are negligible (a usually good approximation). This is why SFG is forbidden in the bulk of most substances, but it is allowed at the interface between bulk phases where there can be no centrosymmetry.

Figure 2.1 shows a simple geometry for SFG that is commonly used. Here, the visible and IR beams are moving in the same direction along the x axis (copropagating), and all three beams are in the same plane, the plane of incidence. The ω_1 and ω_2 beams are either S- or P-polarized; S means the electric field of the light beam is perpendicular to the plane of incidence (along the y axis), and P means the field is in the plane of incidence (the xz plane). The signal-beam polarization is also set to S or P by the polarizer before the beam reaches the detector. The combination of polarizations of all three beams is given by a sequence of three letters, each being S or P (e.g., SSP), with the letters having the following meaning: polarization of the SFG beam, visible beam, and IR beam, respectively. The polarization settings